2007년 2월

석사학위 논문

A Study on Integrity Assessment for Pipelines of Nuclear Power Plants Using Artificial Intelligence

조 선 대 학 교 대 학 원

원 자 력 공 학 과

황 인 준

A Study on the Integrity Assessment for Pipelines of Nuclear Power Plants Using Artificial Intelligence

-인공지능 방법을 이용한 원전 배관의 건전성 평가에 관한 연구-

2007년 2월 23일

조 선 대 학 교 대 학 원

원 자 력 공 학 과

황 인 준

A Study on the Integrity Assessment for Pipelines of Nuclear Power Plants Using Artificial Intelligence

지도교수 나 만 균

이 논문을 원자력공학 석사학위신청 논문으로 제출함

2006년 10월

조 선 대 학 교 대 학 원

원 자 력 공 학 과

황 인 준

황인준의 석사학위 논문을 인준함

위원장 조선대학교 교 수 김 숭 평 인

위원 조선대학교 교 수 나 만 균 인

위원 조선대학교 조교수 김 진 원 인

2006년 11월 30일

조선대학교 대학원

CONTENTS

List of Figures

List of Tables

Abstract

A Study on Integrity Assessment for Pipelines of Nuclear Power Plants Using Artificial Intelligence

Hwang In Joon
지도 교수 : 나 만 균
조선대학교 일반대학원 원자력공학과

곡관은 원자력발전소의 배관 시스템의 중요한 요소로 여겨지고 있다. 이는 배관시스템에서 발생하는 앵커반력(anchor reaction force)을 감소나, 3차원 배치(isometric routing)의 수정에 관계하고 있기 때문이다. 하지만 발전소에서의 곡관은 수많은 열화기구(degradation mechanism)에 직면하고 있고 때문에 다양한 운전조건에서 붕괴에 대한 안전 마진이 정확히 측정되어야 한다.

본 연구에서는 Fuzzy Model 과 Support Vector Machines(SVMs)을 사용하여 다양한 조건들에서 붕괴모멘트를 비선형적이고 시변적인 문제들에 대하여 성공적으로 사용되었다. 감육배관의 붕괴거동은 Subtractive clustering methods에 최적화된 Fuzzy Model과 유전자 알고리즘으로부터 최적화된 SVMs를 통하여 평가되었다.

Fuzzy Model과 Support Vector Regression(SVRs)모델은 유한요소 모델로부터 얻은 수치데이터에 의하여 개발 적용되었고, 훈련 최적화를 위하여 준비된 데이터 셋(Fuzzy Model-training data, SVRs-training, optimization data)으로부터 최적화 되었다. 또한 나머지데이터들은 개발된 모델의 검증을 위하여 시험데이터(test data)로써 사용되었다. 평가 모델들은 각각의 특성을 가지고 있는 세 가지 데이터 셋(extrados, intrados, crawn defect)에 대하여 개발되었다.

이에 대한 붕괴모멘트의 상대 RMS 오차는 Fuzzy Model이 훈련데이터에 대하여 0.5397%, 시험데이터는 0.8673%로 나타났고, SVRs 모델이 훈련 데이터에 대하여 0.2333%, 최적화데이터에 대하여 0.5229%, 그리고 시험데이터에 대하여 0.5011%로 나타났다.

이러한 결과로부터 SVRs 모델이 Fuzzy Model보다 감육배관에 대한 정확한 평가를 위해 사용되기에 충분한 정확도를 가지고 있음을 알 수 있었다.

I. Introduction

The pipe bends and elbows are regarded as critical components in piping systems because they are incorporated into piping systems to allow modification of the isometric routing and more importantly pipe bends are usually incorporated to reduce anchor reaction forces. Also, the pipe bends and elbows are capable of absorbing considerably large thermal expansion and seismic movement through the energy dissipation as a result of local plastic deformation so that they maintain the integrity of piping system under transiently loading conditions [1]. However, care must be taken to ensure that the collapse load is avoided. Therefore, it is important to accurately estimate the safety margin for a collapse of pipe bends and elbows under various operating conditions.

However, the pipe bends and elbows in nuclear power plants are subjected to various degradation mechanisms. Especially, the wall thinning is considered as an important degradation mechanism in carbon steel elbows [2]. The wall-thinned defect is mainly caused by flow-accelerated corrosion, and it results in reducing failure pressure, load-carrying capacity, deformation ability, and fatigue resistance of pipe bends and elbows. Therefore, it is necessary to investigate the effect of wall-thinned defect on the failure behavior of pipe bends and elbows and to accurately estimate the collapse loads of wall-thinned bends and elbows under various loading conditions.

The objective of this thesis is to predict the collapse moment under a variety of loading conditions by a fuzzy inference system and the support vector machines(SVMs) using the measured defect geometry and is to compare with these two models.

Many artificial intelligence techniques including neural networks and fuzzy inference methods have been successfully applied to a lot of nuclear engineering problems such as signal validation [3-5], plant diagnostics [6,7], optimal fuel loading [8,9], control [10], event identification [11,12], and so forth. Also, the

fuzzy identification methods have been largely and successfully applied to system identification problems that will be used in this thesis. Therefore, the fuzzy models are applied in this thesis. The fuzzy model identification can be accomplished through clustering of numerical data. A subtractive clustering method is used as the basis of a fast and robust algorithm for identifying the fuzzy model.

Principal component analysis (PCA) [13-15] is usually used to reduce the dimension of an input space without losing a significant amount of information. Also, PCA has the characteristics to reduce the excessive sensitivity of the fuzzy model to input variable change. Fuzzy system parameters are trained by two methods. A genetic algorithm is applied to optimize the membership function parameters and a least-squares algorithm to optimize the consequent parameters of the fuzzy model.

SVMs have been applied for function classification problems. However, along with the introduction of Vapnik's -insensitive loss function [16], SVMs also have been extended and widely used to solve nonlinear regression estimation problems. In SVM regression the concept is to map the input data into a high dimensional feature space and subsequently carry out the linear regression in the feature space. In this thesis, the SVM regression is used to estimate the collapse loads of wall-thinned bends and elbows under various loading conditions. A genetic algorithm optimizes some related parameters of SVMs so that the SVM regression model has good estimation performance.

To train and test the fuzzy model, and also, to solve the support vectors and test the support vector regression (SVR) model, the collapse moment-related data should be provided. These data are obtained by performing finite element analyses (FEAs) for various loading conditions and defect geometries such as the thinning defect locations of extrados, intrados and crown, bend radius, bend angle, wall thickness at the thinning defect, thinning length, thinning angle, internal pressure, and bending modes of closing and

opening. The collapse moment is predicted using these loading conditions and defect geometries as the inputs into the two models.

II. Calculation of the Collapse Moment Using FEA

In order to evaluate the collapse moment of wall-thinned pipe bends, the nonlinear three-dimensional finite element analysis is performed. Fig. 1 depicts the finite element meshes used in the analysis. Twenty node solid elements with a reduced integration order are used to model the bend and pipes. Considering geometrical symmetry, one forth of the bend is modeled for the intrados and extrados wall-thinning defects and a half of the bend is modeled for a crown wall-thinning defect. The pipe bend is discretised with 8 elements along the straight pipe, 14 elements along the bend, 3 elements across the pipe thickness, and 20 elements along the circumference for the quarter model and 40 elements along the circumference for the half model. The end of the straight pipes is end-capped by a beam to apply a bending moment and an internal pressure; this is modeled by two layers of solid elements. The bending moment is applied as an in-plane rotational displacement to the artificial center node that is assigned a multipoint constraint at the end plane of the beam. Thus, the moment and end-rotation can be obtained from the reaction moment and rotational displacement at this node. The internal pressure is applied to the inner surface of the bend, straight pipe, and end-capped beam as a distributed load.

According to prior studies, the collapse moment of pipebends and elbows containing crack-like defects depends on mesh patterns [17,18]. But a gross structural behavior of defect-free pipe bends and elbows does not strongly depend on mesh patterns [19]. Considering the characteristic of wall-thinning defects which have a smooth three-dimensional shape as shown in Fig. 1, it is expected that the gross behavior of wall-thinned pipe bends is similar to that of defect-free pipe bends rather than cracked pipe bends. Thus, compared to the finite element analyses for the collapse of defect-free pipe bends [19,20], the mesh patterns used for this study would be sufficient to evaluate the collapse

behavior of wall-thinning pipe bends and elbows.

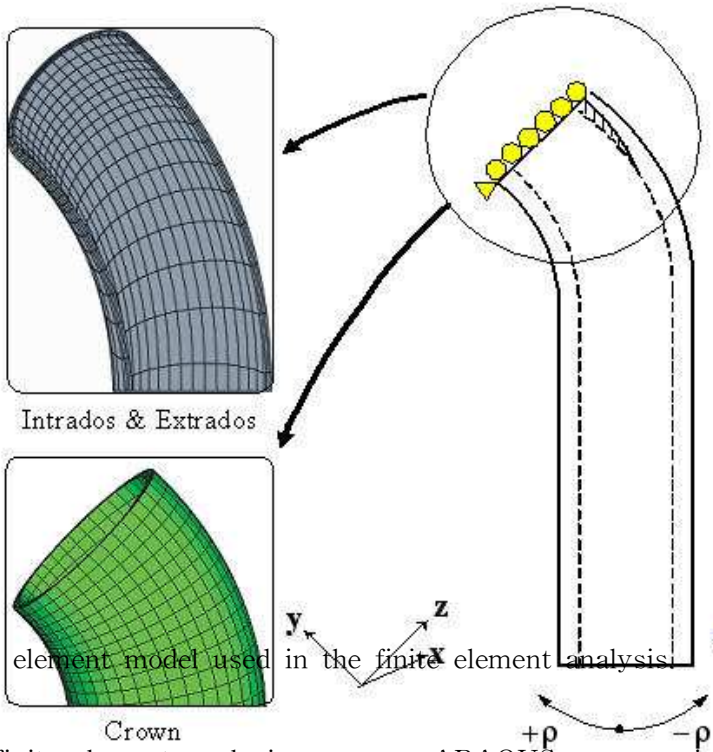

Fig. 1. Finite element model used in the finite element analysis.

General-purpose finite element analysis program, ABAQUS program is used for this study. A former finite element analysis showed that the consideration of geometrical nonlinearity in the finite element analysis is very important for precise determination of pipe bend deflection under various combinations of the closing and opening mode bending and internal pressure [19]. Therefore, both geometric and material nonlinearity are considered in this analysis. The yield stress and ultimate tensile stress of selected material of the bend and attached pipes are 302MPa and 450MPa, and the elastic modulus and the Poisson ratio are 206GPa and 0.3, respectively. Fig. 2 shows a true stress-true strain curve used in the analysis.

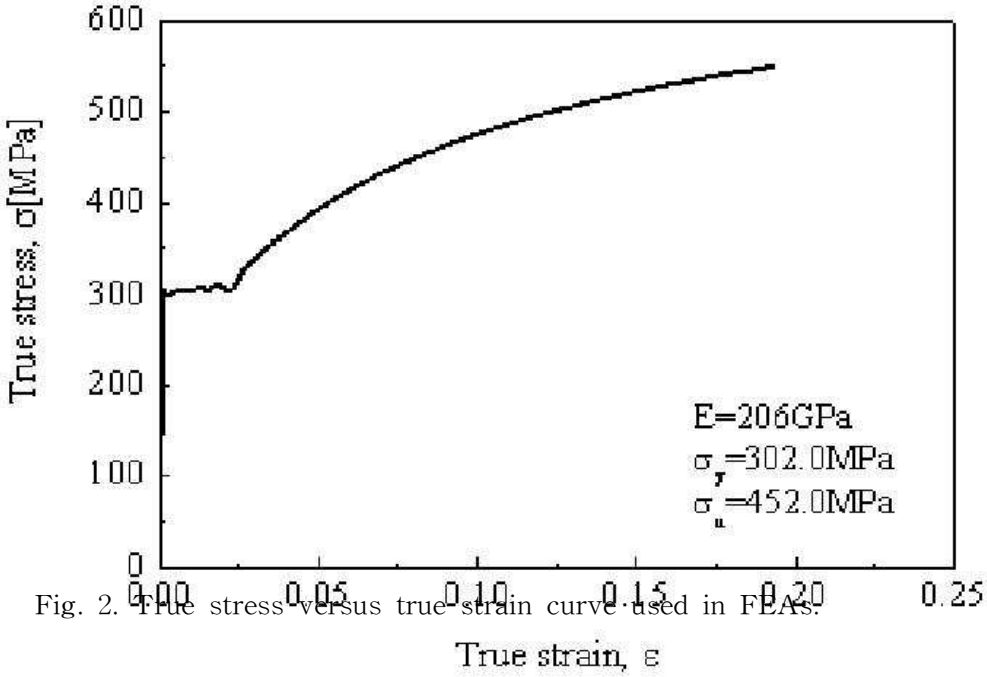

Fig. 2. True stress versus true strain curve used in FEAs.

A. Analysis condition

The carbon steel bends that have outer radius ( ) of 400mm and nominal thickness ( ) of 20mm are selected for the analysis. The bend angle ( ) and bend radius ratio ( ) considered are 30°, 60°, and 90° and 3 and 6, respectively (refer to Fig. 3). The bends and elbows are connected to straight pipes with lengths equal to ten times the mean radius ( ) of the bend to permit free ovalization of end section of the bends. The wall-thinning defects are located at the intrados and extrados centerlines of the pipe bend, and the axial and circumferential shapes of defects are circular.

D_o t_{nom} ϕ R_b/R_m R_m

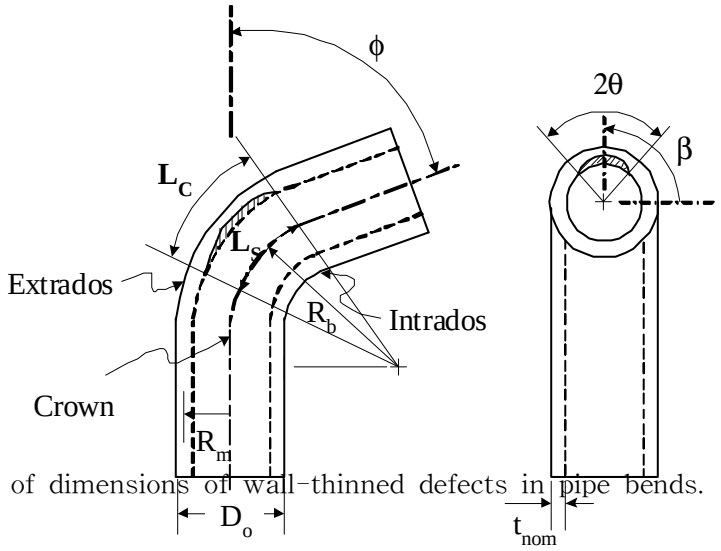

Fig. 3 Definition of dimensions of wall-thinned defects in pipe bends.

Table 1. Analysis conditions for wall-thinned pipe bends.

Thinning Location	Bend Radius ( )	Bendigle (deg)	Defect Geometry			Load	
						Bending Mode	Pressure [MPa]
Extrados Intrados	3.0 R_b/R_m 6.0	30 60	0.25 0.5 1.0 1.5 2.0	0.233 L_s/D_o 0.466 0.699	0.0625 0.125 $\frac{t_{nom}-t_p}{t_{nom}}$ 0.25 0.50	Closing θ/π Opening	0 5 10 15 20

In the analysis, various loading conditions and defect geometries are considered as summarized in Table 1. In the table, t_p is the minimum thickness of the thinned area, L is the equivalent thinning length, and θ is the circumferential half angle of the thinning defect. The combined internal pressure and bending loads are considered as an applied load. An internal pressure of 0 to 20 MPa is used, and either closing- or opening-mode in-plane bending is applied at a constant internal pressure.

B. Collapse Moment

The collapse moment of the bends subjected to in-plane bending can be defined by various methods. In this study, the collapse moment ( ) of the bends was obtained using the twice-elastic slope (TES) method from the M_c moment ( ) versus rotation curve ( ), as illustrated in Fig. 4. This method is the easiest to use, its results are the most reproducible [17,18], and also it is recommended by ASME. When the intersection between TES line and moment versus rotation curve was located beyond the maximum moment, the collapse moment was defined as maximum moment. M ρ

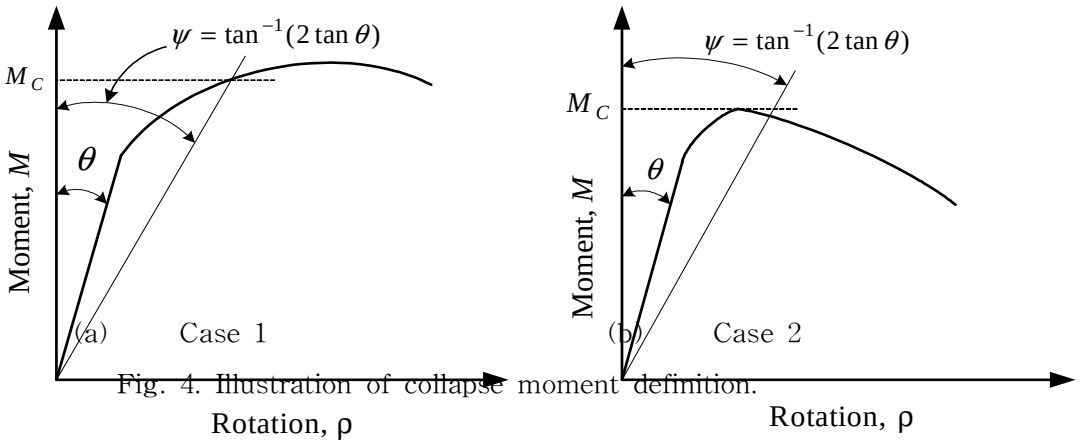

Fig. 4. Illustration of collapse moment definition.

III. Prediction Model Using Artificial Intelligence

In this study, both the fuzzy model based on a subtractive clustering method and the SVM regression model optimized by genetic algorithm are used to predict the collapse moment of the wall-thined pipe bends

A. Fuzzy Model

1. Principal Component analysis

PCA is usually used to reduce the number of input variables into the fuzzy models. The lower dimensional input space has a merit to reduce the time necessary to train the fuzzy models. PCA can facilitate the selection of the input signals to the fuzzy inference system. Also, PCA has the characteristics to reduce the excessive sensitivity of the fuzzy models to input variable change because it has the characteristics of smoothing signals and eliminating noises. In this thesis, the main purpose of PCA application is to reduce the sensitivity.

PCA is to map a multi-dimensional data set into a lower dimensional space while minimizing the loss of information. The basic idea is to project the original space onto a lower dimensional linear subspace spanned by the eigenvectors of the covariance matrix corresponding to the largest eigenvalues. Given a set of signals where is a matrix of which elements consist of samples of signals, its true covariance matrix is replaced with the sample covariance matrix because it is seldom known. The eigenvalues and the orthonormal eigenvectors of the covariance matrix are calculated, and then the eigenvalues are arranged according to their magnitude, . The respective eigenvectors are called the principal components. The eigenvalues are proportional to the amount of variance (information) represented by the corresponding principal component. The transformation to the principal component space can be written as:

$\boldsymbol{X}$ $\boldsymbol{X} = [\boldsymbol{x}_1\ \boldsymbol{x}_2\ \cdots\ \boldsymbol{x}_p]$ $n \times p$ $\boldsymbol{X}$ n p $\boldsymbol{S}$ $\boldsymbol{Z}$ $\boldsymbol{S}$

$\lambda_1 \geq \lambda_2 \geq \cdots \geq \lambda_p$ $\boldsymbol{p}_1, \boldsymbol{p}_2, \cdots, \boldsymbol{p}_p$

,

$$Z = XP \tag{1}$$

where $Z = [z_1, z_2, \cdots, z_m]$ and $P = [p_1, p_2, \cdots, p_m]$.

The feature matrix, Z, can be transformed back into the original data X without a loss of information as long as the number of features, m, is equal to the dimension of the original space, p. For $m < p$, some information is usually lost. The objective is to choose a small m that does not lose much information. In this thesis, the feature vector that is calculated by Eq. (1) is used as input to the fuzzy model.

2. Subtractive clustering based fuzzy model

A fuzzy model based on a subtractive clustering method is used to predict the collapse moment of the wall-thinned pipe bends. The fuzzy model is constructed from a collection of fuzzy *if-then* rules. The inputs and outputs of the fuzzy model are real-valued variables. Therefore, instead of considering the Mamdani (1975) type fuzzy if-then rules that requires time-consuming defuzzification calculation, a Takagi-Sugeno (1985) type fuzzy inference system is used where the i-th fuzzy rule for k-th time instant data is described as follows:

$$\textit{If } x_1(k) \textit{ is } A_1^i \textit{ AND} \cdots \textit{AND } x_m(k) \textit{ is } A_m^i(k), \\ \textit{then } y^i \textit{ is } f^i(x_1(k), \cdots, x_m(k)), \tag{2}$$

where $x_j(k)$ is the input linguistic variable to the fuzzy inference system (j = 1, 2, $\cdots$, m; m = the number of input variables), $A_j^i(k)$ the membership function of the j-th input variable for the antecedent of the i-th fuzzy rule (i = 1, 2, $\cdots$, n; n = the number of rules), and $y^i(k)$ the output of the i-th fuzzy rule. In Eq. (2), the *if* part is fuzzy linguistic, while the *then* part is crisp.

The fuzzy model identification can be accomplished through clustering of numerical data. A subtractive clustering (SC) method is used as the basis of a fast and robust algorithm for identifying a fuzzy model [21] and assumes the

availability of input/output training data where $(\boldsymbol{x}^T(k), y(k))$ N. It is assumed that the data points have been normalized in each dimension. The method starts by generating a number of clusters in the $m \times N$ dimensional input space. The SC method considers each data point as a potential cluster center and uses a measure of the potential of each data point, which is defined as a function of the Euclidean distances to all other input data points [21]:

$$P(k) = \sum_{j=1}^{N} e^{-4\|\boldsymbol{x}(k)-\boldsymbol{x}(j)\|^2/r_\alpha^2}, \quad k = 1,2,\ldots,N \tag{3}$$

where r_α is a radius, defining a neighborhood, which has considerable influence on the potential. Obviously, the potential of a data point is high when it is surrounded by many neighboring data.

The procedure of the subtractive clustering includes the following steps:

(i) After the potential of every data point has been computed by Eq. (3), the data point with the highest potential is selected as the first cluster center. Let $\boldsymbol{x}^*(1)$ be the location of the first cluster center and $P^*(1)$ be its potential value.

(ii) An amount of potential is subtracted from each data point as a function of its distance from the chosen cluster center. The data points near the cluster center will have greatly reduced potential, and therefore are unlikely to be selected as the next cluster center. In general, after the i-th cluster center has been obtained, the potential of each data point is revised by the following equation:

$$P(k) := P(k) - P^*(i)\, e^{-4\|\boldsymbol{x}(k)-\boldsymbol{x}^*(i)\|^2/r_\beta^2}, \quad k = 1,2,\ldots,N \tag{4}$$

where $\boldsymbol{x}^*(i)$ is the location of the i-th cluster center and $P^*(i)$ is its potential value. r_β is also a radius, usually greater than r_α in order to limit the number of generated clusters. When the potential of all data points

have been revised according to Eq. (4), the data point with the highest potential (after this subtraction) is selected as the next cluster center.

(iii) If the inequality $P^*(i) < \varepsilon P^*(1)$ is true, these calculations stop, else these calculations are repeated. The parameter ε is a design parameter, which controls the number of generated clusters which is the number of fuzzy rules, n.

When the cluster estimation method is applied to a collection of input/output data, each cluster center is in essence a prototypical data point that exemplifies a characteristic behavior of the system and each cluster center can be used as the basis of a fuzzy rule that describes the system behavior. Therefore, a complete fuzzy system identification algorithm can be developed based on the results of the SC technique. A number of Takagi-Sugeno type fuzzy rules can be generated, where the premise parts are fuzzy sets, defined by the cluster centers that are obtained by the SC algorithm. The membership function of an input data vector $\boldsymbol{x}(k)$ to a cluster center $\boldsymbol{x}^*(i)$ can be defined as follows:

$$A^i(\boldsymbol{x}(k)) = e^{-4 \| \boldsymbol{x}(k) - \boldsymbol{x}^*(i) \|^2 / r_\alpha^2}, \tag{5}$$

The fuzzy inference system output $A^i(\boldsymbol{x}(k))$ is calculated by the weighted average of the consequent parts of the fuzzy rules as follows:

$$\hat{y}(k) = \frac{\sum_{i=1}^{n} A^i(\boldsymbol{x}(k)) f^i(\boldsymbol{x}(k))}{\sum_{i=1}^{n} A^i(\boldsymbol{x}(k))}. \tag{6}$$

The function $\hat{y}(k)$ is a polynomial in the input variables, but it can be any function as long as it can appropriately describe the output of the fuzzy inference system within the fuzzy region specified by the antecedent of the rule. When the fuzzy rule output is of the following form:

$$f^i(\boldsymbol{x}(k))$$

$$f^i(\boldsymbol{x}(k)) = \sum_{j=1}^{m} q_{ij} x_j(k) + r_i \quad , \tag{7}$$

where

q_{ij} = weighting value of the j-th input on the i-th fuzzy rule output,

r_i bias of the i-th fuzzy rule output,

the fuzzy inference system is called a first-order Takagi-Sugeno (1985) type fuzzy model since the output of an arbitrary i-th fuzzy rule, f^i, is represented by the first-order polynomial of inputs as given in Eq. (7).

Therefore, the output of the fuzzy model given by Eq. (6) can be rewritten as

$$\hat{y}(k) = \sum_{i=1}^{n} \overline{w^i}(k) f^i(\boldsymbol{x}(k)) = \boldsymbol{w}^T(k)\boldsymbol{q} \quad , \tag{8}$$

where

$$\overline{w^i}(k) = \frac{A^i(\boldsymbol{x}(k))}{\sum_{i=1}^{n} A^i(\boldsymbol{x}(k))} \quad ,$$

$$\boldsymbol{q} = [q_{11} \cdots q_{n1} \cdots \cdots q_{1m} \cdots q_{nm}\ r_1 \cdots r_n]^T \quad .$$

The value $\overline{w^i}(k)$ is the normalized firing level of the i-th fuzzy rule. For a series of input/output data pairs, the following equation is derived from Eq. (8):

$$\hat{\boldsymbol{y}} = \boldsymbol{W}\boldsymbol{q} \quad , \tag{9}$$

where

$$\hat{\boldsymbol{y}} = [\hat{y}(1)\ \hat{y}(2) \cdots\ \hat{y}(N)]^T$$

$$\boldsymbol{W} = [w(1)\ w(2) \cdots\ w(N)]^T$$

$\boldsymbol{q}$ $\boldsymbol{W}$

output of the fuzzy model is represented by the $N\times(m+1)n$-dimensional matrix $\boldsymbol{W}$ and the $(m+1)n$-dimensional parameter vector $\boldsymbol{q}$.

3. Fuzzy model optimization

The fuzzy model should be optimized to accomplish the desired performance. The optimization is accomplished by a genetic algorithm combined with a least-squares method. The genetic algorithm is used to optimize the cluster radii, r_a and r_b, for the subtractive clustering of numerical data, and the least squares algorithm is used to calculate the consequent parameters, q_{ij} and r_i.

Compared to the conventional optimization methods that move from one point to another, genetic algorithms start from many points simultaneously climbing many peaks in parallel. Accordingly, genetic algorithms are less susceptible to being stuck at local minima than conventional search methods [22,23]. Also, the genetic algorithm is the most useful method to solve optimization problems with multiple objectives. In genetic algorithms, the term chromosome refers to a candidate solution that minimizes a cost function, generally encoded as a bit string. As the generation proceeds, populations of chromosomes are iteratively altered by biological mechanisms inspired by natural evolution such as selection, crossover, and mutation. The genetic algorithms require a fitness function that assigns a score to each chromosome (candidate solution) in the current population, and maximize the fitness function value. The fitness function evaluates the extent to which each candidate solution is suitable for specified objectives.

The problem of learning a smooth mapping from data samples is ill-posed in the sense that the reconstructed mapping is not unique. Constraints can be imposed to the mapping to make the problem well-posed. Typical constraints are smoothness and piecewise smoothness. This method to exchange an ill-posed problem into a well-posed one is called regularization [24,25].

Regularization is a well-known method for the treatment of mathematically ill-posed problems. It has been applied successfully to numerous machine learning problems including the avoidance of overfitting in neural network training. In this thesis, the regularization is accomplished by making the fuzzy model have smaller consequent parameters, which causes the fuzzy model to respond smoother and less likely to overfit. In this thesis, the specified multiple objectives are to minimize a root mean squared error along with the small consequent parameters. Therefore, the following multiple objectives are suggested:

$$, \tag{10}$$

where and are the weighting coefficients, and and have a concept of energy defined as

$$F = \exp(-\mu_1 E_1 - \mu_2 E_2) \tag{11}$$

$$\mu_1 \quad \mu_2 \quad , \quad E_1 \quad E_2$$

$$E_1 = \sqrt{\frac{1}{N}\sum_{k=1}^{N}(y(k)-\hat{y}(k))^2} \tag{12}$$

The variables and denote the actual measured signal and the signal estimated by the fuzzy model, respectively. is the number of consequent parameters, and , that is, the number of the elements of the vector . is introduced for the regularization of the input. The smaller the consequent parameters, better is generalization capability of the fuzzy model. The fitness function depends strongly on the relative value of . The ratio is iteratively altered in the training stage by the values of and so that the best chromosome with the maximum fitness keeps the specified relative magnitude of two terms of and in Eq. (10).

$$E_2 = \sqrt{\frac{\boldsymbol{q}^T\boldsymbol{q}}{L}}$$

$y(k)$ $\hat{y}(k)$ L q_{ij} r_i $\boldsymbol{q}$ E_2

Since the genetic algorithm requires much computational time if there are many parameters involved, the genetic algorithm is combined with a least-squares algorithm. If some parameters of the fuzzy model are fixed by the

μ_2/μ_1 E_1 E_2

μ_2/μ_1

$\mu_1 E_1$ $\mu_2 E_2$

genetic algorithm, the resulting fuzzy model output can be described as a series of expansions of some basis functions. This basis function expansion is linear in its adjustable parameters as shown in Eq. (8) since has been known by the genetic algorithm. Therefore, the least-squares method can be used to determine the consequent parameters. The consequent parameters are chosen to minimize the following cost function including the squared error between the target output and the estimated output :

$$J = \frac{1}{2}(\boldsymbol{y} - \hat{\boldsymbol{y}})^2 \tag{13}$$

where .

The solution to minimize the above cost function can be obtained by

$$\boldsymbol{y} = [y(1)\ y(2)\ \cdots\ y(N)]^T \tag{14}$$

The parameter vector in Eq. (14) can be solved easily by using the pseudo-inverse of the matrix .

Figure 5 shows the automatic optimization procedure of the fuzzy model

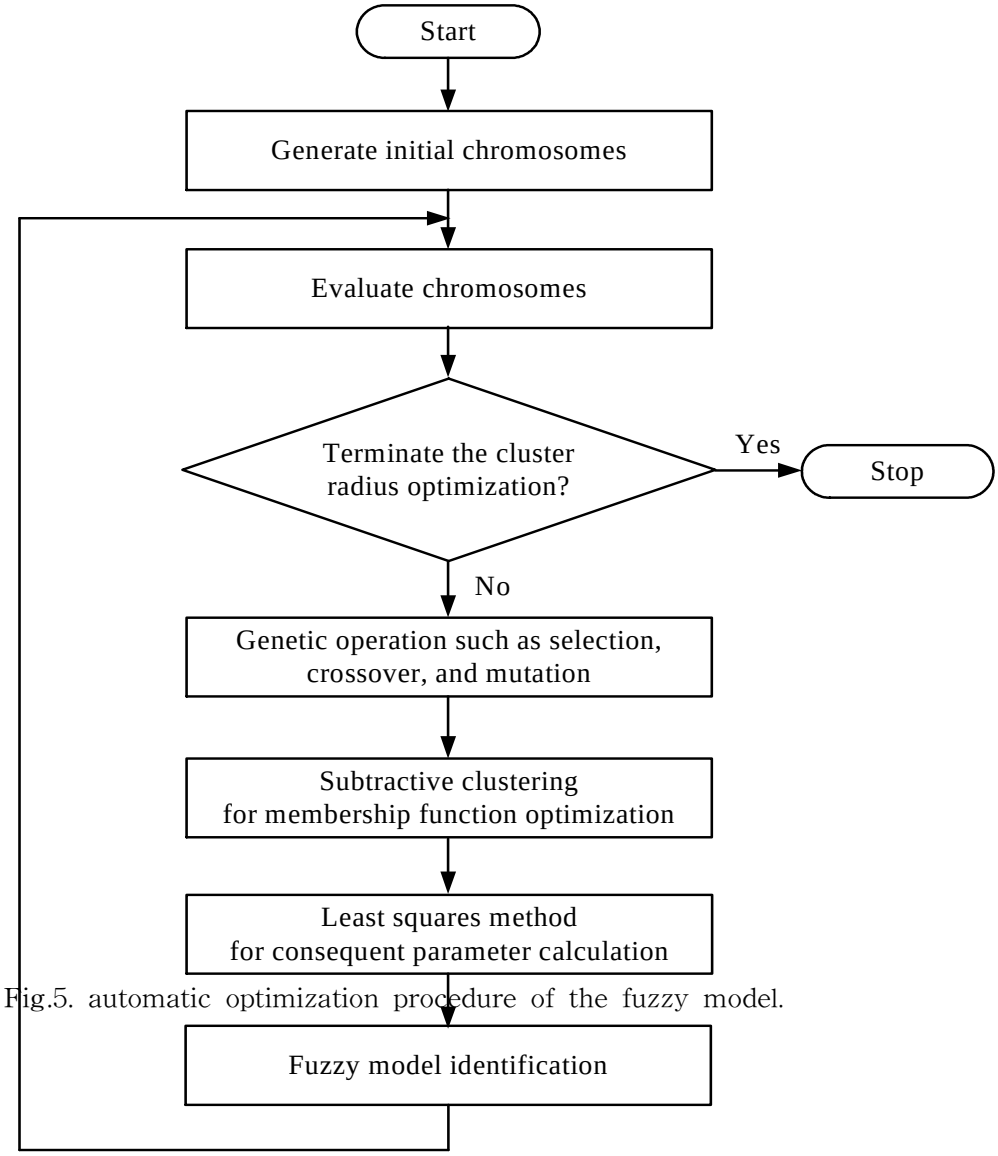

Fig.5. automatic optimization procedure of the fuzzy model.

B. SVR Models

A relatively new promising method for learning separating functions in pattern recognition problems or for performing functional estimation in regression problems is the support vector machine. SVMs represent novel learning techniques that have been introduced in the framework of structural risk minimization (SRM). That is, unlike classical adaptation algorithms that work in an L_1 or L_2 norm and minimize the absolute value of an error or of an error square, the SVM performs SRM. In this way, it creates a regression model with the expected probability of error for regression problems, which means good performance on unseen data. This property is of particular interest to the soft computing field because the model that generalizes well is a good model and not the model that performs well on training data pairs [26].

1. SVR Models

In general regression learning problems, the learning machine is given training data, from which it attempts to learn the input-output relationship. The basic concept of the SVM regression is to nonlinearly map the original data into a higher dimensional feature space. Hence, given a set of data $\{(\boldsymbol{x}_i, y_i)\}_{i=1}^{N}$ where $\boldsymbol{x}$ is the input vector to support vector machines, y_i is the actual output value and N is the total number of data patterns, the SVM regression function considers approximation functions of the form

$$y = f(\boldsymbol{x}) = \sum_{i=1}^{N} w_i \phi_i(\boldsymbol{x}) = \boldsymbol{w}^T \boldsymbol{\phi}(\boldsymbol{x}) + b \quad (15)$$

where $\boldsymbol{x}_i$ is called the feature that is nonlinearly mapped from the input space $\boldsymbol{x}$, $\phi_i(\boldsymbol{x})$, and $\boldsymbol{w} = [w_1\, w_2 \cdots\ w_N]^T \quad \boldsymbol{\phi} = [\phi_1\ \phi_2 \cdots\ \phi_N]^T$. The support vector weight $\boldsymbol{w}$ and a bias b are calculated by minimizing the following regularized risk function:

$$R(\boldsymbol{w}) = \frac{1}{2}\boldsymbol{w}^T\boldsymbol{w} + \lambda \sum_{i=1}^{N} L_\epsilon(\boldsymbol{x}_{i,} y_{i,} f) \quad (16)$$

where

$$L_\epsilon(\boldsymbol{x}, y, f) = |y - f(\boldsymbol{x})|_\epsilon = \begin{cases} 0 & |y - f(\boldsymbol{x})| < \epsilon \\ |y - f(\boldsymbol{x})| - \epsilon & otherwise \end{cases} \tag{17}$$

Here, ϵ and λ are user-specified parameters and $L_\epsilon(\boldsymbol{x}, y, f)$ is called the ϵ-insensitive loss function (refer to Fig. 6) [16]. The loss is equal to zero if the difference between the estimated $f(\boldsymbol{x})$ and the measured value is less than an error level ϵ. Vapnik's ϵ-insensitive loss function defines an ϵ tube (see Figs. 6 and 7). If the estimated value is within the tube, the loss is zero. Note that for $\epsilon = 0$, Vapnik's ϵ-insensitive loss function is equivalent to the absolute error (L_1 norm) function.

The regularized risk function can be rewritten by the following constrained form:

$$R(\boldsymbol{w}, \boldsymbol{\xi}, \boldsymbol{\xi}^*) = \frac{1}{2}\boldsymbol{w}^T\boldsymbol{w} + \lambda \sum_{i=1}^{N} (\xi_i + \xi_i^*) \tag{18}$$

under constraints

$$\begin{cases} y_i - \boldsymbol{w}^T\boldsymbol{\phi}(\boldsymbol{x}) - b \le \epsilon + \xi_i, & i = 1, 2, \cdots, N \\ \boldsymbol{w}^T\boldsymbol{\phi}(\boldsymbol{x}) + b - y_i \le \epsilon + \xi_i^*, & i = 1, 2, \cdots, N \\ \xi_i, \xi_i^* \ge 0, & i = 1, 2, \cdots, N \end{cases} \tag{19}$$

where the constant λ determines the trade-off between the flatness of $f(x)$ (the weights vector norm) and the amount up to which deviations larger than ϵ are tolerated, and ξ_i and ξ_i^* are slack variables representing the upper and lower constraints on the outputs of the system, respectively. Both slack variables are positive values.

$$\boldsymbol{\xi} = [\xi_1\ \xi_2\ \cdots\ \xi_N]^T \qquad \boldsymbol{\xi}^* = [\xi_1^*\ \xi_2^*\ \cdots\ \xi_N^*]^T$$

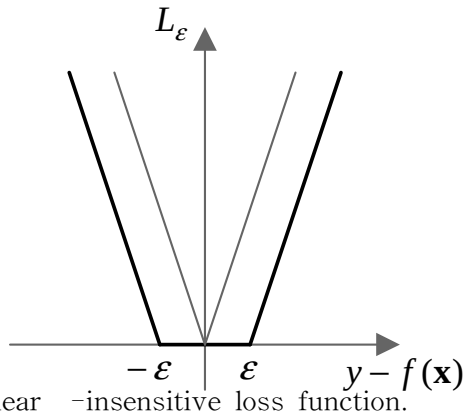

Fig. 6. Linear -insensitive loss function.

ϵ

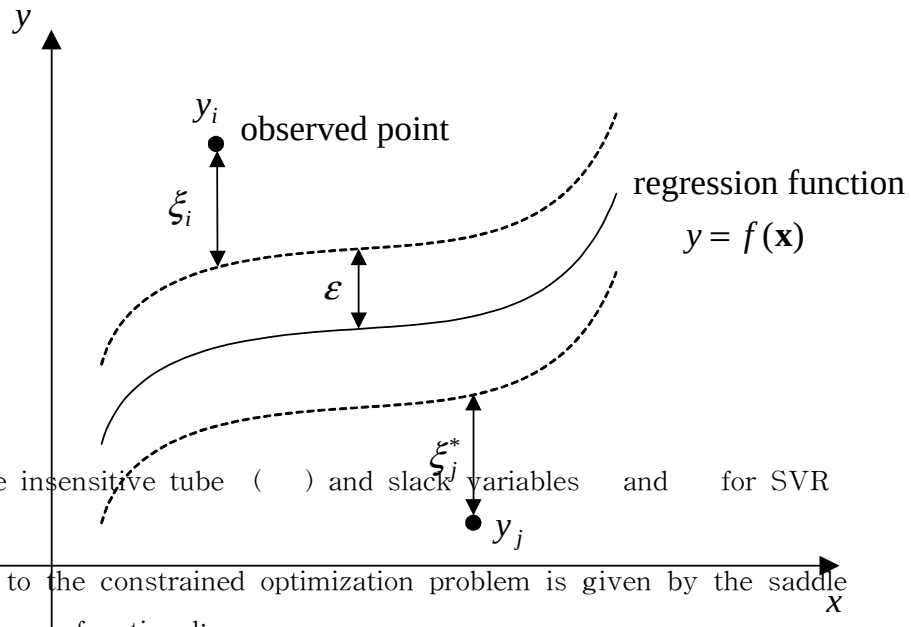

Fig. 7 . The insensitive tube ( ) and slack variables and for SVR

The solution to the constrained optimization problem is given by the saddle point of the Lagrange functional:

$\pm\epsilon$ $\boldsymbol{\xi}$ $\boldsymbol{\xi}^*$

$$\phi(\boldsymbol{w},b,\xi_i,\xi_i^*,\alpha_i,\alpha_i^*,\beta_i,\beta_i^*) = \frac{1}{2}\boldsymbol{w}^T\boldsymbol{w} + \lambda\sum_{i=1}^{N}(\xi_i+\xi_i^*) - \sum_{i=1}^{N}\alpha_i[\boldsymbol{w}^T\boldsymbol{\phi}(\boldsymbol{x}_i)+b-y_i+\epsilon+\xi_i]$$
$$- \sum_{i=1}^{N}\alpha_i[y_i-\boldsymbol{w}^T\boldsymbol{\phi}(\boldsymbol{x}_i)-b+\epsilon+\xi_i] - \sum_{i=1}^{N}(\beta_i\xi_i+\beta_i^*\xi_i^*) \quad (20)$$

The above equation is minimized with respect to the primal variables , and then maximized with respect to the nonnegative Lagrangian multipliers . The minimum with respect to of the Lagrange functional provides the following conditions:

$\boldsymbol{w}, b, \xi_i, \xi_i^*$ $\alpha_i, \alpha_i^*, \beta_i, \beta_i^*$ $\boldsymbol{w}, b, \xi_i, \xi_i^*$

, (21)

$$\boldsymbol{w} = \sum_{i=1}^{N}(\alpha_i - \alpha_i^*)\boldsymbol{\phi}(\boldsymbol{x}_i)$$

,

$$\sum_{i=1}^{N}(\alpha_i-\alpha_i^*) = 0$$

.

$$\lambda - \alpha_i - \beta_i = 0, \quad i = 1,2,\cdots,N$$

The Lagrange functional can be rewritten by using the above minimum conditions as follows:

$$\lambda - \alpha_i^* - \beta_i^* = 0, \quad i = 1,2,\cdots,N$$

,

(22)

$$\Psi(\alpha_i,\alpha_i^*) = \sum_{i=1}^{N} y_i(\alpha_i-\alpha_i^*) - \epsilon\sum_{i=1}^{N}(\alpha_i+\alpha_i^*) - \frac{1}{2}\sum_{i=1}^{N}\sum_{j=1}^{N}(\alpha_i-\alpha_i^*)(\alpha_j-\alpha_j^*)\boldsymbol{\phi}^T(\boldsymbol{x}_i)\boldsymbol{\phi}(\boldsymbol{x}_j) \quad (23)$$

under constraints

By solving the above equation with standard quadratic programming technique, the values of are found out. By substituting Eq. (21) into Eq. (15), the regression function becomes

$$\begin{cases} \sum_{i=1}^{N}(\alpha_i-\alpha_i^*) = 0 \\ 0 \le \alpha_i \le \lambda, \quad i = 1,2,\cdots,N \\ 0 \le \alpha_i^* \le \lambda, \quad i = 1,2,\cdots,N \end{cases}$$

, (24)

α_i, α_i^*

$$y = f(\boldsymbol{x}) = \sum_{i=1}^{N}(\alpha_i-\alpha_i^*)\boldsymbol{\phi}^T(\boldsymbol{x}_i)\boldsymbol{\phi}(\boldsymbol{x}) + b = \sum_{i=1}^{N}(\alpha_i-\alpha_i^*)K(\boldsymbol{x},\boldsymbol{x}_i) + b$$

where $K(\boldsymbol{x}, \boldsymbol{x}_i) = \boldsymbol{\phi}^T(\boldsymbol{x}_i)\boldsymbol{\phi}(\boldsymbol{x})$ is called the kernel function. A number of coefficients $\alpha_i - \alpha_i^*$ are nonzero values and the corresponding training data points have approximation error equal to or larger than ϵ. They are called support vectors. The bias b is calculated as

$$b = \frac{1}{2}\sum_{i=1}^{N}(\alpha_i - \alpha_i^*)(K(\boldsymbol{x}_r, \boldsymbol{x}_i) + K(\boldsymbol{x}_s, \boldsymbol{x}_i)), \quad (25)$$

where $b =$ and $\boldsymbol{x}_r$ and $\boldsymbol{x}_s$ are support vectors.

The two most relevant design parameters for the SVR model are the insensitivity zone ϵ and the regularization parameter λ. An increase of the constant λ penalizes larger errors, which leads to a decrease of approximation error. This can also be achieved only by increasing the weights vector norm. However, an increase in the weight vector norm does not make sure of the good generalization performance of a model. An increase in the insensitivity zone ϵ means a reduction in requirements for the accuracy of approximation and it also decreases the number of support vectors, leading to data compression. An increase in ϵ has smoothing effects on modeling highly noisy polluted data.

2. *Genetic optimization*

The SVR model is obtained by learning from experimental data and should be optimized to maximize the estimation performance. The experimental data are divided into three kinds of data sets such as the training data, the optimization data, and the test data. The training data is used to solve the coefficients $\alpha_i - \alpha_i^*$ and the bias b in Eq. (24). The optimization data is used to optimize the design parameters of SVR models by a genetic algorithm and to determine an additional parameter for sampling the training data. The test data is used to verify the developed SVR models.

Regarding the selection of the training data from all the given data, since a

lot of data cluster on the mean value of the collapse moment and they are less informative, each data point that is located far away from the mean value has a high probability of being selected for the training data. That is, a random number r_k is generated for each data point and if this random number satisfies the following relationship, the data point is selected as the training data:

$$\begin{cases} \textit{selected as training data}, & \text{if } r_k < \sqrt{\dfrac{|y_k|}{\max_k\{|y_k|\}}} + p,\ k = 1, \cdots, N \\ \textit{not selected as training data}, & \textit{otherwise} \end{cases} \tag{26}$$

where r_k is a uniformly distributed random number, y_k the normalized collapse moment that has zero mean value, and the parameter p that affects the number of the training data is determined by the genetic algorithm. The optimization data is elected every six time from the remaining data that the training data is excluded. That is, the optimization data set comprises four fifth of the remaining data pairs that the training data is excluded and the test data set consists of the remaining data.

The optimization is accomplished by a genetic algorithm suitable for a multi-objective function. The genetic algorithm is used to optimize the insensitivity zone ε, the regularization parameter λ, the sharpness of the radial basis kernel function to be used in this thesis, and an additional parameter (p in Eq. (26)) for sampling the training data from the acquired data. These parameters are not completely independent but affect one another. These parameters are optimized so that the fitness function below is maximized.

Since the genetic algorithm optimizes four parameters, each chromosome has four parameters encoded as a bit string. In this thesis, the specified multiple objectives are to minimize a root mean squared error along with the small maximum error. Therefore, the following multiple objectives are suggested:

$$F = \exp(-\mu_1 E_1 - \mu_2 E_2 - \mu_3 E_3 - \mu_4 E_4) \quad (27)$$

where μ_1, μ_2, μ_3 and μ_4 are the weighting coefficients, and E_1, E_2, E_3 and E_4 have a concept of energy defined as

$$E_1 = \sqrt{\frac{1}{N_t}\sum_{k=1}^{N}(y_t(k) - \hat{y_t}(k))^2} \quad (28)$$

$$E_2 = \sqrt{\frac{1}{N_o}\sum_{k=1}^{N_o}(y_o(k) - \hat{y_o}(k))^2} \quad (29)$$

$$E_3 = \max_k\{y_t(k) - \hat{y_t}(k)\} \quad (30)$$

$$E_4 = \max_k\{y_o(k) - \hat{y_o}(k)\} \quad (31)$$

The variables $y(k)$ and $\hat{y}(k)$ denote the FEA output and the output estimated by the SVR model, respectively. The subscripts, t and o, indicate the training data and the optimization data, respectively and N_t and N_o represent the numbers of the training data and the optimization data. Fig. 8 shows the automatic optimization procedures of the SVR model.

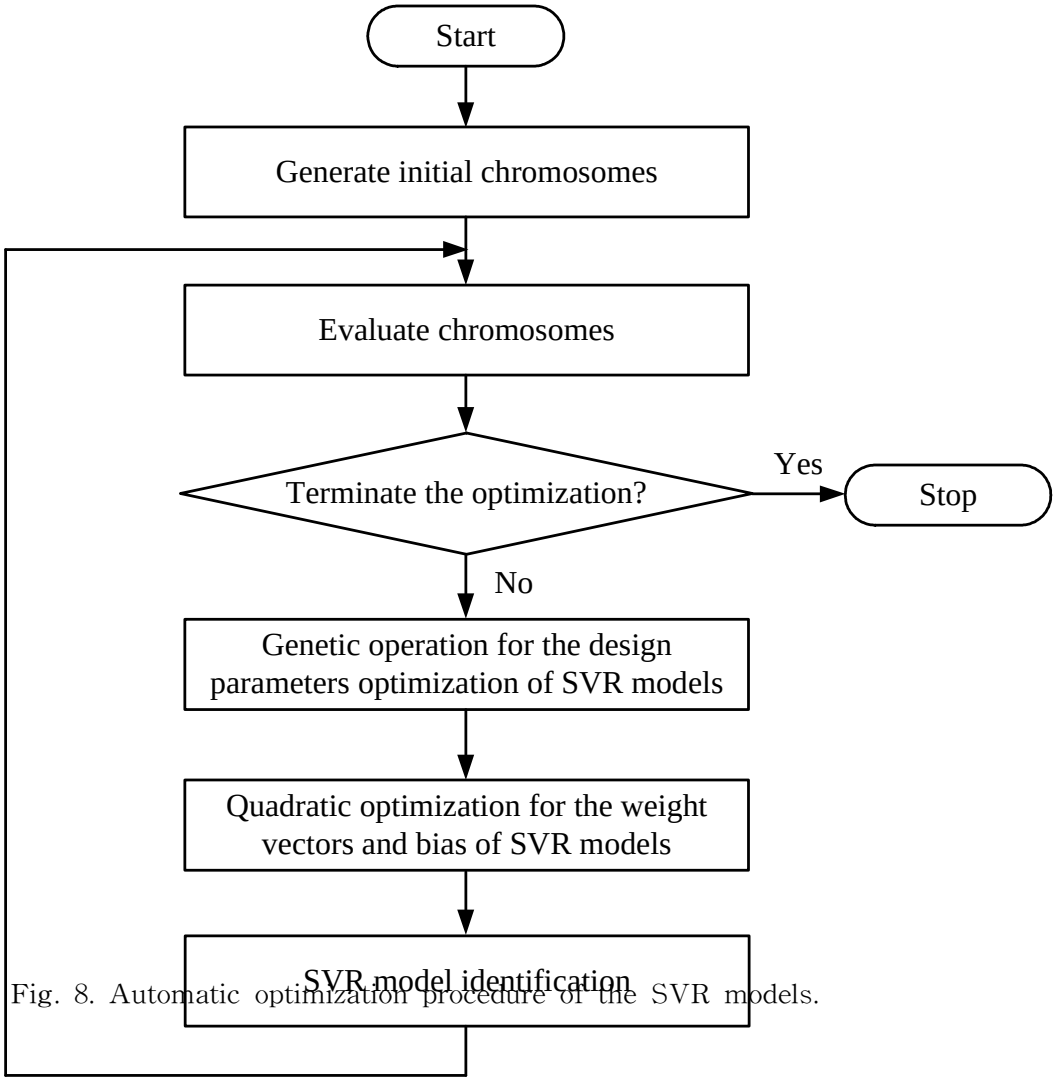

Fig. 8. Automatic optimization procedure of the SVR models.

IV. Application to the Collapse Moment Estimation

First of all, necessary data have to be prepared to devise fuzzy model and SVR models for estimating the collapse moment of wall-thinned pipe bends and elbows. Since the sufficient related field data of nuclear power plants did not exist, as described in Chapter 2, finite element analyses were performed to provide the data needed for developing the each models for each loading condition and defect geometry case.

In this study, the ranges of the input signals for models are described in Table 1. The provided data consist of a total of 3712 input-output data pairs composed of 1700 extrados defect location cases, 1700 intrados cases, and 312 crown cases. The characteristic of the collapse moment is much different according to the three wall-thinned defect locations of extrados, intrados, and crown, which is represented by $(x_1, x_2, \cdots, x_8, y)$. Therefore, the data are classified into the three classes of defect locations and three models are designed for the three classes, respectively. The input signals, x_1 through x_8, indicate the bend radius, bend angle, wall thickness at the thinning defect, thinning length, thinning angle, internal pressure, and bending modes of closing and opening, respectively. y is the FEA output which indicates the collapse moment.

A. Fuzzy Model

The three fuzzy models are trained for three kinds of data sets divided into the extrados, intrados and crown defect locations, respectively, which has smaller errors compared with results using only one data set. The numbers of rules of the three fuzzy models are automatically determined by the subtractive clustering method. The antecedent parameters such as membership function parameters are determined through cluster radius optimization by the genetic algorithm and the consequent parameters and are optimized by the least-squares method. The inputs to the fuzzy models are preprocessed by PCA and the transformed input signals are applied to the fuzzy models.

Figure 9 shows the estimation error histograms of the training and test data for an extrados defect location. The relative RMS errors are 0.5476% for the training data and 0.8095% for the test data. Figure 10 shows the estimation error histograms of the training and test data for an intrados defect location. The relative RMS errors are 0.5035% for the training data and 0.9354% for the test data. Figure 11 shows the estimation error histograms of the training and test data for a crown defect location. The relative RMS errors are 0.6717% for the training data and 0.7841% for the test data. Although a little difference is found out among the RMS errors of the three defect locations, their estimation performances are almost similar. Figure 12 shows the collapse moment histograms and the target and estimated collapse moment, and also their estimation errors of the training and test data in case that the three extrados, intrados, and crown defects are considered together. The relative RMS errors are 0.5397% for the training data and 0.8673% for the test data. From this figure, it is shown that although the maximum error is large at some defect cases, the maximum error can decrease if the defect conditions change a little during the collapse moment monitoring.

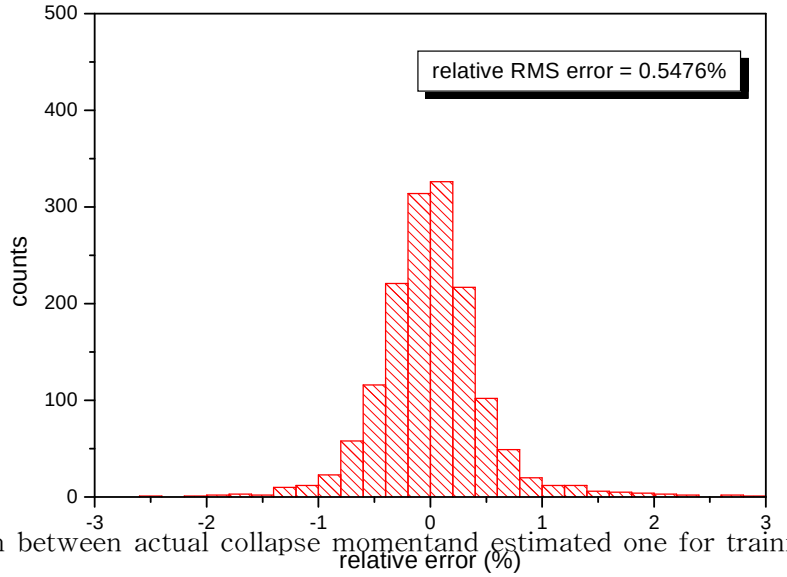

(a) Error histogram between actual collapse momentand estimated one for training data

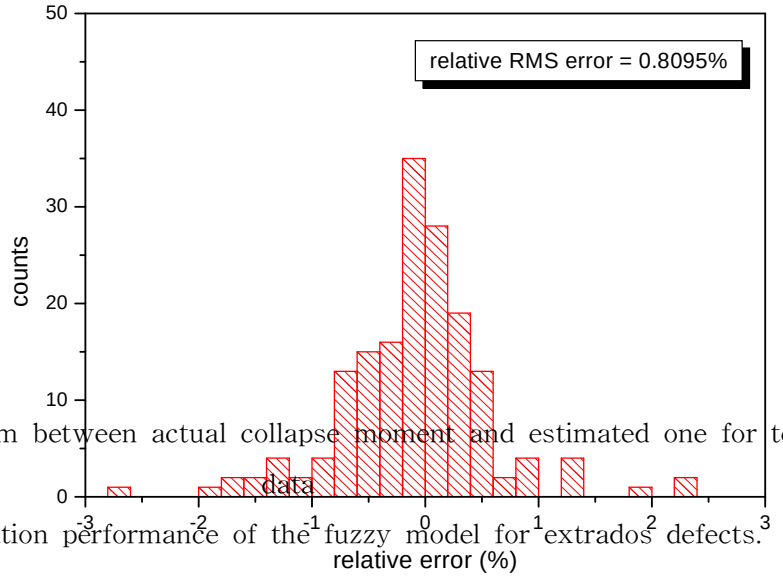

(b) Error histogram between actual collapse moment and estimated one for test data

Fig. 9. Estimation performance of the fuzzy model for extrados defects.

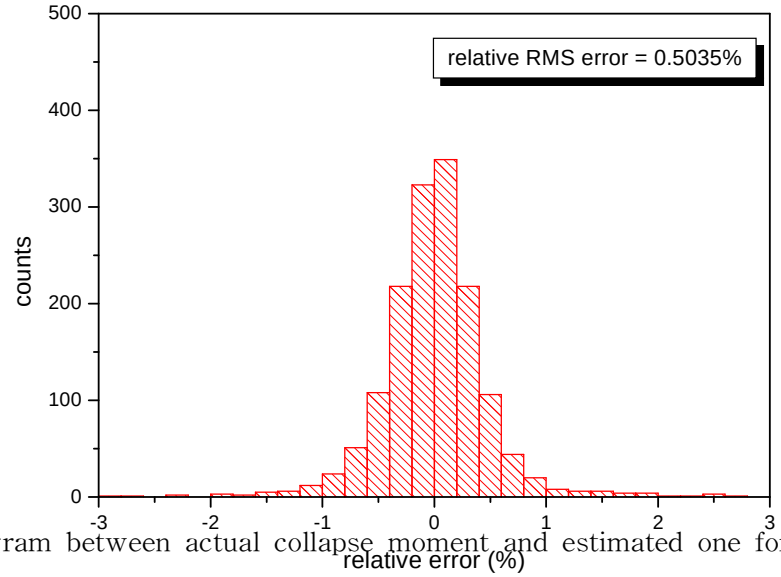

(a) Error histogram between actual collapse moment and estimated one for training data

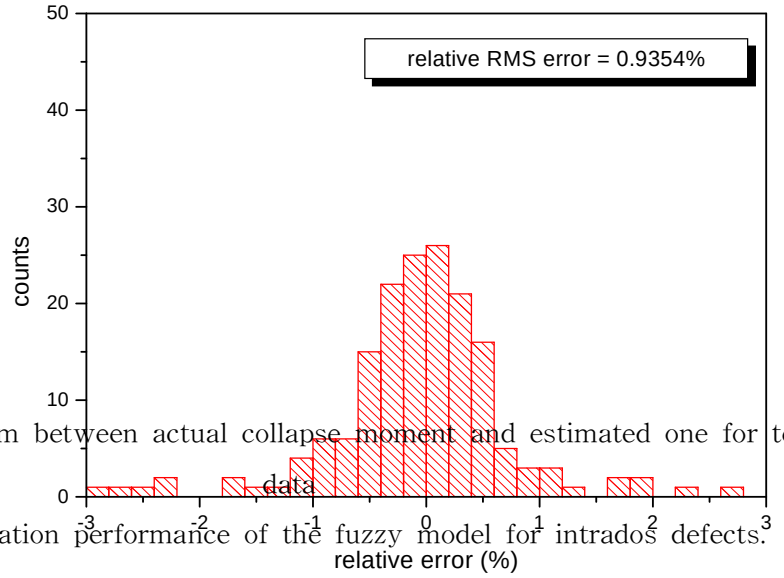

(b) Error histogram between actual collapse moment and estimated one for test data

Fig. 10. Estimation performance of the fuzzy model for intrados defects.

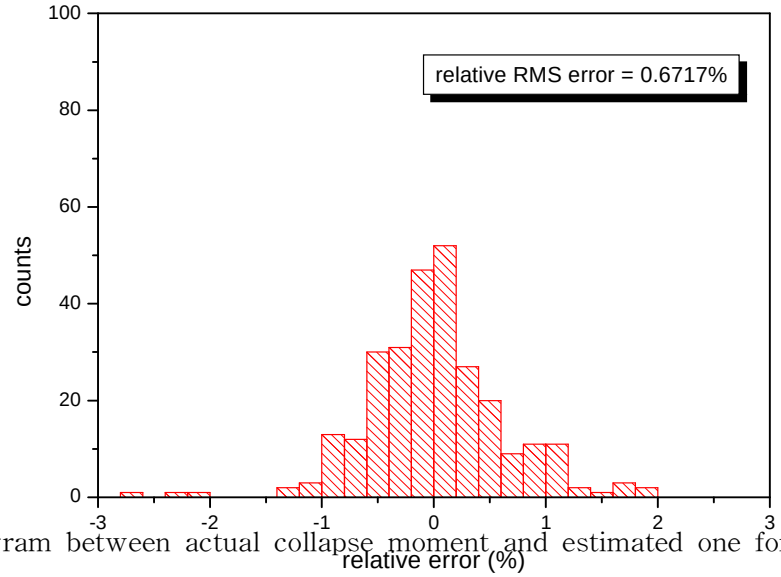

(a) Error histogram between actual collapse moment and estimated one for training data

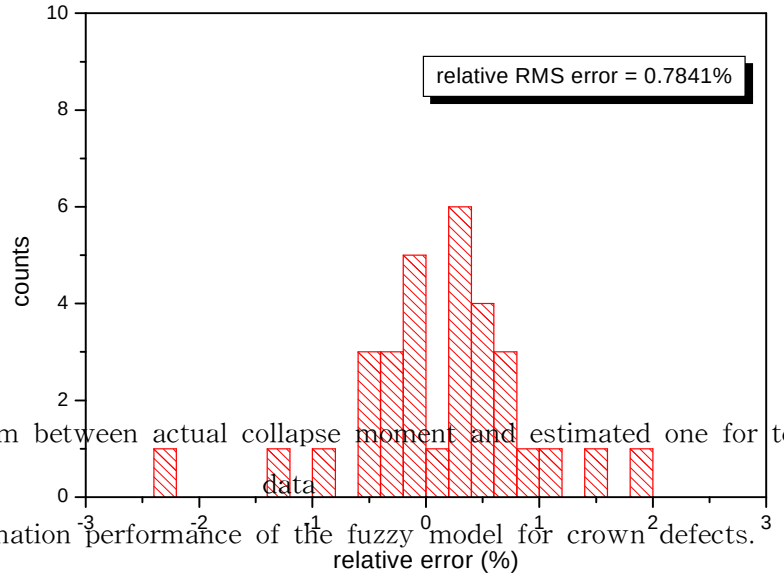

(b) Error histogram between actual collapse moment and estimated one for test data

Fig. 11. Estimation performance of the fuzzy model for crown defects.

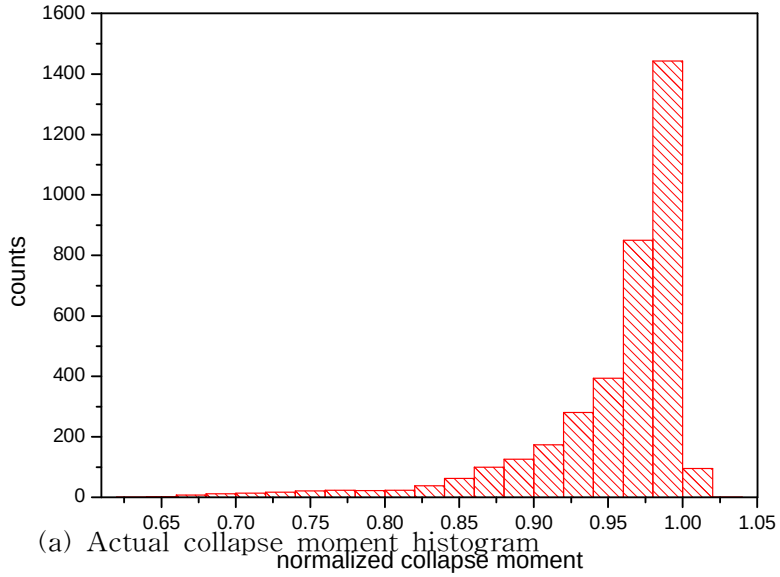

(a) Actual collapse moment histogram

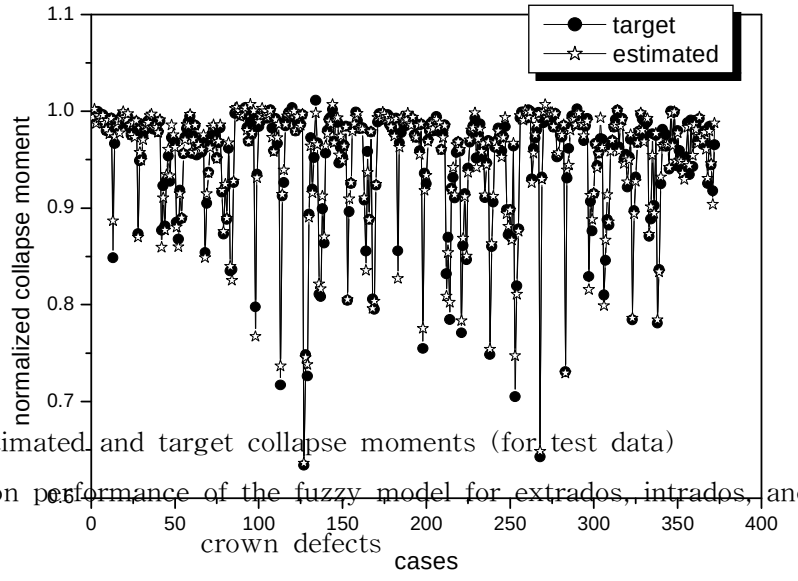

(b) Estimated and target collapse moments (for test data)

Fig. 12. Estimation performance of the fuzzy model for extrados, intrados, and crown defects

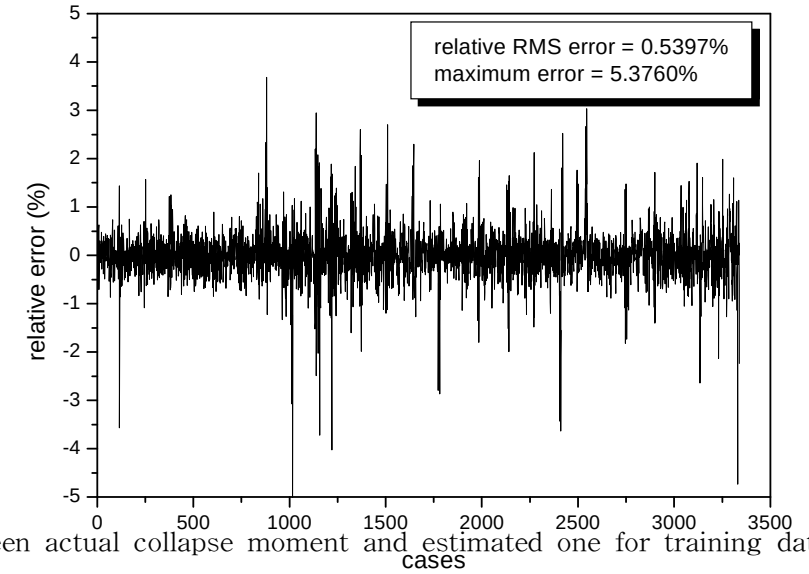

(c) Errors between actual collapse moment and estimated one for training data

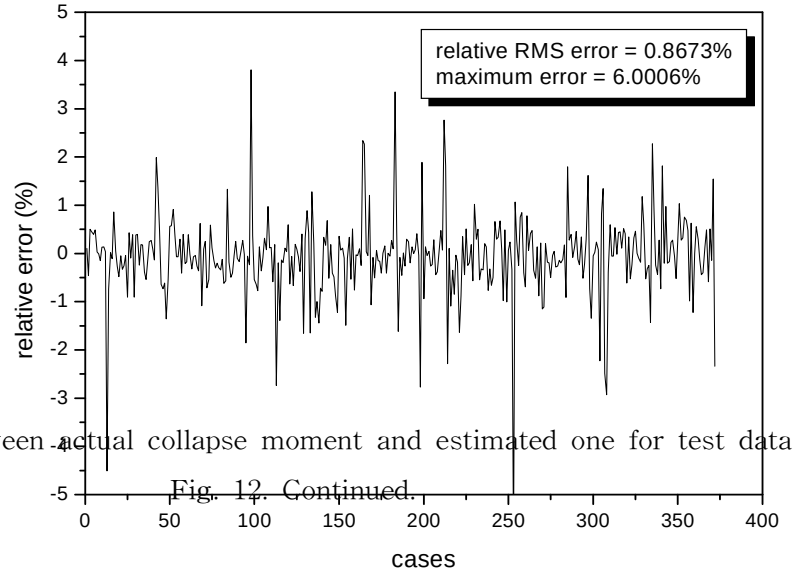

(d) Errors between actual collapse moment and estimated one for test data

Fig. 12. Continued.

Table 2 summaries the estimation results of collapse moments by the fuzzy models. The fuzzy models have similar estimation performance for the three defect locations. Also, it is known that the RMS error of the fuzzy models for the test data is only a little greater than the RMS error for the training data. Therefore, if the fuzzy neural networks are trained first using data for a variety of loading conditions and defect geometry cases, they can accurately estimate the collapse moment for any other defect cases.

Table 2. Estimation results of collapse moment by the fuzzy model.

		Extrados defects	Intrados defects	Crown	Total
fitness		0.9462	0.9504	0.9344	
Number of rules (input)		40(7)	54(7)	5(6)	
Training data	Relative maximum error (%)	5.3760	3.6368	4.7385	5.3760
	Relative RMS error (%)	0.5476	0.5035	0.6717	0.5397
Test data	Relative maximum error (%)	4.5134	6.0006	2.3344	6.0006
	Relative RMS error (%)	0.8095	0.9354	0.7841	0.8673

B. SVR model

In the SVR models, the inputs are normalized so that they have a standard deviation of one and a mean of zero and the normalized input signals are applied to the SVR models. The kernel functions used in this thesis are the following radial basis functions:

$$K(\boldsymbol{x}, \boldsymbol{x_i}) = \exp\left(-\frac{(\boldsymbol{x}-\boldsymbol{x_i})^T(\boldsymbol{x}-\boldsymbol{x_i})}{2\sigma^2}\right) \quad (32)$$

The (SVR) models are optimized by a genetic algorithm with chromosomes of which components consists of the insensitivity zone ε, the regularization parameter C, and the sharpness (σ) of the radial basis kernel function of the SVR models, and an additional parameter (p in Eq. (26)) for sampling the training data from the acquired data.

Fig. 13 shows the collapse moment histograms and the target and estimated collapse moment, and also their estimation errors of the training data, the optimization data, and test data in case that the three extrados, intrados, and crown defects are considered together.

Table 3 summaries the estimation results of collapse moments by the SVR models. The SVR models have similar estimation performance for the three defect locations. The relative RMS errors are 0.2333% for the training data, 0.5229% for the optimization data, and 0.5011% for the test data and the maximum error is 2.8641%. Also, it is known that the RMS error magnitude of the SVR models for the test data is almost similar to that for the optimization data. Therefore, if the SVR models are optimized first using data for a variety of loading conditions and defect geometry cases, they can accurately estimate the collapse moment for any other defect cases.

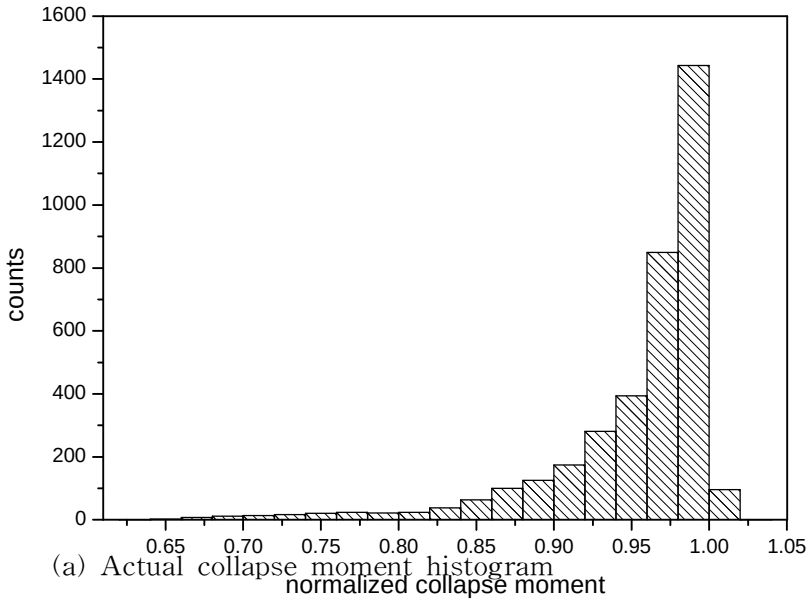

(a) Actual collapse moment histogram

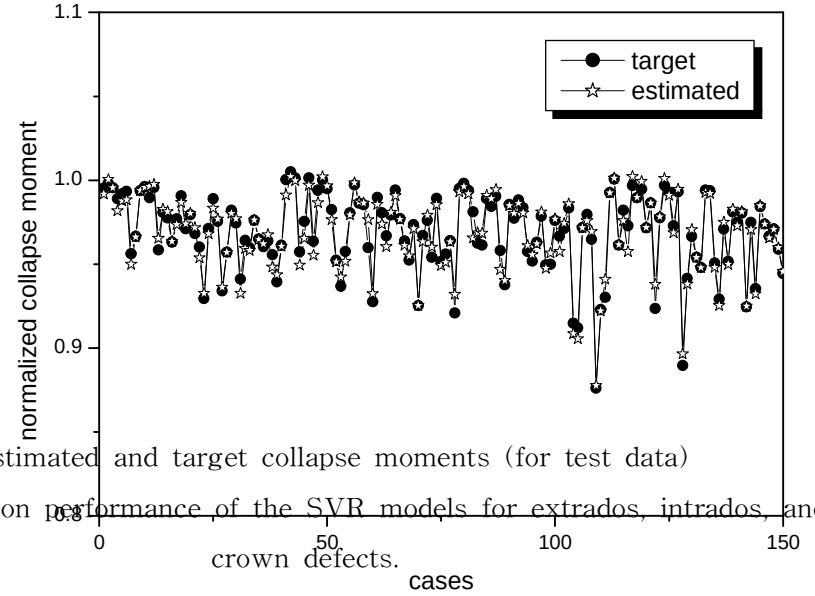

(b) Estimated and target collapse moments (for test data)

Fig. 13. Estimation performance of the SVR models for extrados, intrados, and crown defects.

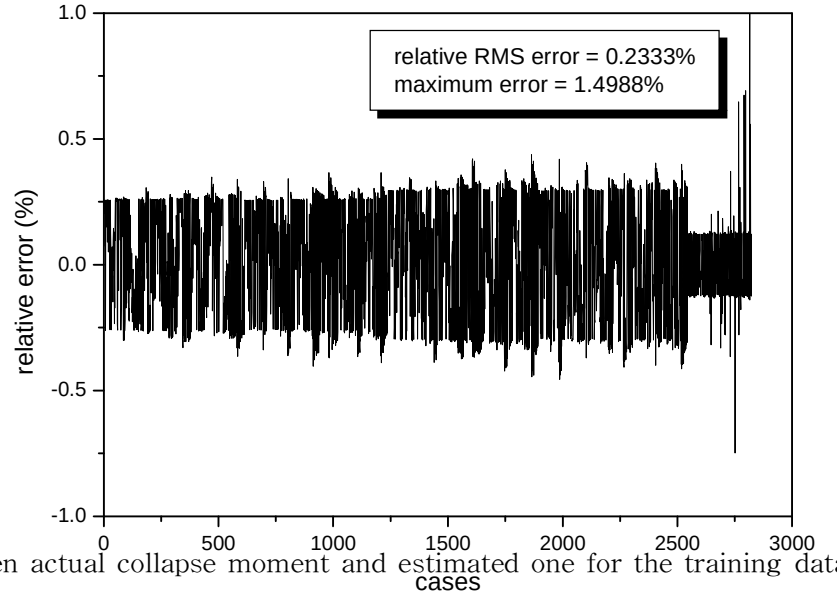

(c) Errors between actual collapse moment and estimated one for the training data

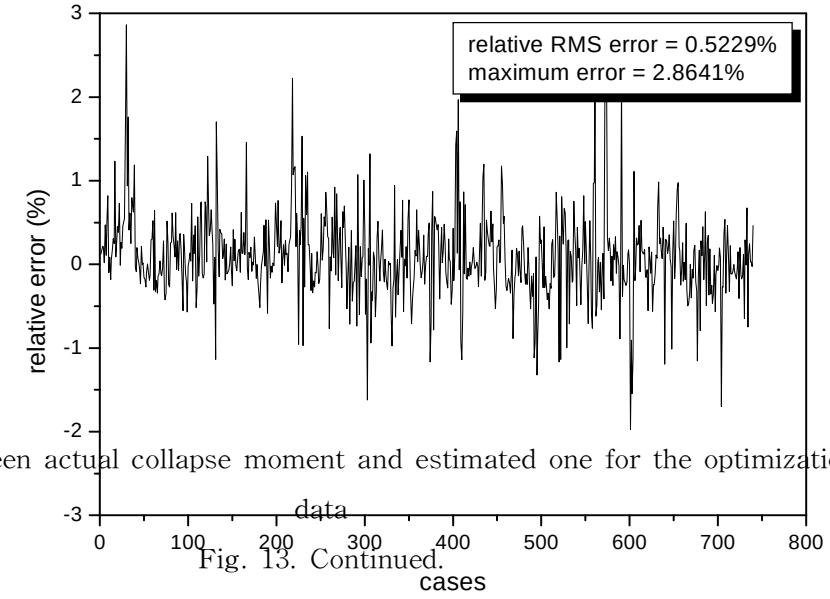

(d) Errors between actual collapse moment and estimated one for the optimization data

Fig. 13. Continued.

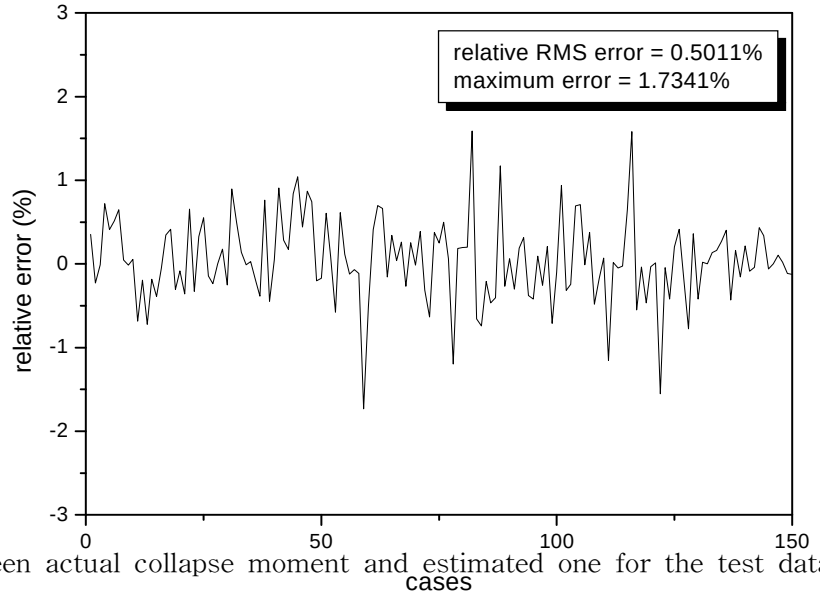

(e) Errors between actual collapse moment and estimated one for the test data

Fig. 13. Continued.

Table 3. Optimized parameters of SVR models.

Parameters Defect location	Insensitivity zone (ϵ)	Regularization parameter(λ)	The sharpness of the radial basis kernel function (σ)	A parameter related to selecting the training data (p)
Extrados	4.7545×10^{-2}	609.34	1.0046	0.4285
Intrados	4.7540×10^{-2}	742.94	1.2546	0.4285
Crown	4.5353×10^{-2}	1723.7	2.7973	0.4798

Table 4. Estimation results of the collapse moments by the SVR models.

Defect location		Extrados	Intrados	Crown	Total
Fitness		0.5592	0.6247	0.8993	-
Number (No.) of support vectors		643	618	194	-
Training data	No.	1236	1307	279	2822
	Relative RMS Error (%)	0.2232	0.2522	0.1782	0.2333
	Relative maximum error (%)	0.4033	0.4558	1.4988	1.4988
Optimization data	No.	386	327	27	740
	Relative RMS Error (%)	0.5031	0.5596	0.2894	0.5229
	Relative maximum error (%)	2.8641	2.4783	0.7488	2.8641
Test data	No.	78	66	6	150
	Relative RMS Error (%)	0.4952	0.5293	0.0850	0.5011
	Relative maximum error (%)	1.7341	1.5878	0.1261	1.7341

V. Conclusion

Two nonlinear regression models using artificial intelligence have been used to estimate the collapse moment due to the wall-thinned defects of bends and elbows in piping systems. The developed models have been applied to the numerical data obtained by the finite element analysis.

In the fuzzy model, the PCA was used to preprocess the input signals to the fuzzy model and the fuzzy models were trained by using the data set prepared for training (training data) and verified by using another data set (test data) different (independent) from the training data. Also, three fuzzy models were trained for three data sets divided into the three classes of extrados, intrados, and crown defects. The relative RMS errors are 0.5397% for the training data and 0.8673% for the test data. The RMS error for the test data is only a little greater than the RMS error for the training data.

In the SVRs model, three SVR models have been developed for three data sets divided into the three classes of extrados, intrados, and crown defects. The SVR models were trained by using the data set prepared for training (training data), optimized by the optimization data set, and verified by using the test data set independent from the training data and the optimization data. The relative RMS errors are 0.5229% for the optimization data and 0.5011% for the test data. The RMS error magnitude of the SVR models for the test data is similar to that for the optimization data.

The collapse moment was well estimated by using thess two methods. Also, it was known in this study that the SVR models can more accurately estimate the collapse moment than the fuzzy model can.

References

[1] Shalaby, M.A., Younan, M.Y.A., 1999. Limit loads for pipe elbows subjected to in-plane opening moments and internal pressure. J. Press. Ves. Tech. 121, 17-23.

[2] Chexal, B., Horowitz, J., Dooley, B., Millett, P., Wood, C., Jones, R., 1998. Flow-accelerated corrosion in power plant, EPRI/TR-106611-R2.

[3] Fantoni, P., Figedy, S. and Racz, A., 1998. A neuro-fuzzy model applied full range signal validation of PWR nuclear power plant data, FLINS-98, Antwerpen, Belgium.

[4] Hines, J.W., Wrest, D.J. and Uhrig, R.E., 1997. Signal validation using an adaptive neural fuzzy inference system, Nucl. Technol. 119(2), 181-193.

[5] Na, M.G., Sim, Y.R., Park, K.H., Lee, S.M., Jung, D.W., Shin, S.H., Upadhyaya, B.R., Zhao, K. and Lu, B., 2003. Sensor monitoring using a fuzzy neural network with an automatic structure constructor. IEEE Trans. Nucl. Sci. 50(2), 241-250.

[6] Bartlett, E.B. and Uhrig, R.E., 1992. Nuclear power plant diagnostics using an artificial neural network, Nucl. Technol. 97, 272-281.

[7] Marseguerra, M. and Zio, E., 1994. Fault diagnosis via neural networks: The Boltzmann machine. Nucl. Sci. Eng. 117(3), 194-200.

[8] Kim, H.G., Chang, S.H. and Lee, B.H., 1993. Optimal fuel loading pattern design using an artificial neural network and a fuzzy rule-based system, Nucl. Sci. Eng. 115(2), 152-163.

[9] Lee, J.H., Sim, H.J., Jang, C.S. and Kim, C.H., 1998. Incorporation of neural networks into simulated annealing algorithm for fuel assembly loading pattern optimization in a PWR, Proc. Int. Conf. on Phys. of Nucl. Sci.and Technol., Oct. 5-8, American Nuclear Society, Long Island, New York, p. 75.

[10] Na, M.G., 1998. Design of a genetic fuzzy controller for the nuclear steam

generator water level control. IEEE Trans. Nucl. Sci. 45(4), 2261-2271.

[11] Bartal, Y., Lin, J. and Uhrig, R.E., 1995. Nuclear power plant transient diagnostics using artificialneural networks that allow "don't-know" classifications, Nucl. Technol. 110(3), 436-449.

[12] Roh, C.H., Chang, H.S., Kim, H.G. and Chang, S.H., 1996. Identification of reactor vessel failures using spatiotemporal neural networks. IEEE Trans. Nucl. Sci. 43(6), 3223-3229.

[13] Chen, J. and Liu, J., 1999. Mixture principal component analysis models for process monitoring, Ind. Eng. Chem. Res. 38(4), 1478-1488.

[14] Na, M.G. and Sim, Y.R., 2001. An input feature selection method applied to fuzzy neural networks for signal estimation. J. Korean Nucl. Soc. 33(5), 457-467.

[15] Wang, X.Z. and Li, R.F., 1999. Combining conceptual clustering and principal component analysis for state space based process monitoring. Ind. Eng. Chem. Res. 38(11), 4345-4358.

[16] Vapnik, V., 1995. The Nature of Statistical Learning Theory. Springer, New York.

[17] Yahiaoui, K., Moffat, D.G., Moreton, D.N., 2000a. Piping elbows with cracks, Part 2: a parametric study of the influence of crack size on limit loads due to pressure and opening bending. J. Strain Anal. 35, 35-46.

[18] Yahiaoui, K., Moffat, D.G., Moreton, D.N., 2000b. Piping elbows with cracks, Part 2: Global finite element and experimental plastic loads under opening bending. J. Strain Anal. 35, 47-57.

[19] Chattopadhyay, J, 2002. The effect of internal pressure on in-plane collapse moment of elbows. Nucl. Eng. & Design 202, 133-144.

[20,] Robertson, A., Li, H., Mackenzie, D., 2005, Plastic collapse of pipe bends under combined internal pressure and in-plane bending. Int. J. Pres. Ves. & Piping 82, 407-416.

[21] Chiu, S.L., 1994. Fuzzy model identification based on cluster estimation, J.

Intell. Fuzzy Systems 2, 267-278.

[22] Goldberg, D.E., 1989. Genetic Algorithms in Search, Optimization and Machine LearningAddison Wesley, Reading, MA.

[23] Mitchell, M., 1996. An Introduction to Genetic Algorithms. MIT Press, Cambridge, MA.

[24] Kumar, P., Merchant, S.N. and Desai, U.B., 2004. Improving Performance in Pulse Radar Detection Using Bayesian Regularization for Neural Network Training, Digital Signal Processing 14, 438-448

[25] Tian, L. and Noore, A., 2005. Evolutionary neural network modeling for software cumulative failure time prediction. Reliability Eng. System Safety 87, 45-51.

[26] Vojislav, K, 2001. Learning and soft computing - support vector machines, neural networks and fuzzy logic models. MIT Press, Cambridge, MA.

감사의 글

먼저 뭐라고 글을 시작해야 할지 망설여집니다.

두려움과 설레임 속에서 시작한 대학원 생활이 벌써 2년. '최선을 다하자', '매 순간을 헛되이 보내지 말자'라고 다짐한 저를 뒤로한 채 어느덧 2007년이 와버렸습니다. 실수, 후회, 방황…. 이러한 시간이 있었기에 제가 있을 수 있다고 생각합니다. 모든일을 함에 있어서 결코 쉬운 것은 없었지만 뒤처지지 않고 무사히 졸업할 수 있게 된 것을 뒤돌아보면 그동안 저에게 많은 지도와 끊임없이 격려해주신 분들이 계셨다는 것을 다시금 생각하게 합니다.

이 논문이 완성되기까지 저 황인준이라는 학생에게 많은 관심과 격려로 처음부터 끝까지 변함없이 따뜻하게 지도해 주신 나만균 교수님께 진심으로 감사드립니다. 항상 저를 걱정해주시고 챙겨주시는 교수님에게 저는 과분할 정도로 많은 애정을 받고 있었다고 생각합니다. 제가 학교를 졸업하고 어느 분야의 어디에 있던지 교수님께서 보여주신 열정과 열의은 잊지 못할 것입니다.

그리고, 항상 따뜻한 애정과 관심을 보여주신 김숭평 교수님, 정운관 교수님, 이경진 교수님, 송종순 교수님, 김진원 교수님, 심홍기 교수님, 송재승 교수님께도 감사의 말씀을 전해드리고 싶습니다.

졸업하기까지 학교생활 잘할 수 있도록 신경써주고 도와준 금주형, 보미누나, 유선이형, 철기형, 대석이형에게 고맙다는 말 해주고 싶습니다.

실험실에서 같이 생활하고, 졸업하고 나서도 신경써주며 항상 안부를 물어주었던 동원이형, 형이 보여줬던 모든것이 저에게는 모두 도움이 됐었다고 말해주고 싶습니다. 그리고 선호형, 장곤이형, 재법이형, 선미에게도 고맙다는 말을 전합니다.

항상 저를 지켜봐 준 주일, 보열, 경열, 민신, 광현 외 98학번 동기들, 항상 최선을 다하는 병선이, 헌영이, 희성이에게 고마움을 전합니다. 함께 지내온 시간이 즐거웠다는 말 전합니다.

또, 학부, 석사생활동안 티격태격하며 같이 지내온 연수야, 고맙다!

끝으로 아낌없는 지원과 믿음으로 지켜봐 주신 부모님과 누나, 동생에게 감사의 마음 전하며 오늘에 만족하지 않고 항상 정진하는 자세를 가지며 살아가도록 하겠습니다.

저작물 이용 허락서

학 과	원자력공학과	학 번	20057117	과 정	석사
성 명	한글: 황 인 준 한문 : 黃 仁 俊 영문 : Hwang In-Joon				
주 소	광주광역시 북구 운암동 미라보아파트 307-201				
연락처	E-MAIL : coolin1207@paran.com				
논문제목	한글: 인공지능 이용을 이용한 배관의 건전성 평가에 관한 연구 A Study on Integrity Assessment for Pipelines of Nuclear Power Plants Using Artificial Intelligence				
	영문:				

본인이 저작한 위의 저작물에 대하여 다음과 같은 조건아래 조선대학교가 저작물을 이용할 수 있도록 허락하고 동의합니다.

- 다 음 -

1. 저작물의 DB구축 및 인터넷을 포함한 정보통신망에의 공개를 위한 저작물의 복제, 기억장치에의 저장, 전송 등을 허락함
2. 위의 목적을 위하여 필요한 범위 내에서의 편집·형식상의 변경을 허락함. 다만, 저작물의 내용변경은 금지함.
3. 배포·전송된 저작물의 영리적 목적을 위한 복제, 저장, 전송 등은 금지함.
4. 저작물에 대한 이용기간은 5년으로 하고, 기간종료 3개월 이내에 별도의 의사 표시가 없을 경우에는 저작물의 이용기간을 계속 연장함.
5. 해당 저작물의 저작권을 타인에게 양도하거나 또는 출판을 허락을 하였을 경우에는 1개월 이내에 대학에 이를 통보함.
6. 조선대학교는 저작물의 이용허락 이후 해당 저작물로 인하여 발생하는 타인에 의한 권리 침해에 대하여 일체의 법적 책임을 지지 않음
7. 소속대학의 협정기관에 저작물의 제공 및 인터넷 등 정보통신망을 이용한 저작물의 전송·출력을 허락함.

동의여부 : 동의(0) 반대( )

2007년 2월 일

저작자: 황 인 준 (서명 또는 인)

조선대학교 총장 귀하